Wave Propagation Modeling Analysis of Earthquake Records for Buildings

Hideji Kawakami*[1] and Mendbayar Oyunchimeg[2]

[1] Professor, Geosphere Research Institute of Saitama University, Japan
[2] Graduate student, Department of Civil and Environmental Engineering, Saitama University, Japan

Abstract

This paper introduces an application of wave propagation modeling to building response investigation. We have analyzed the computed responses of analytical building models and the obtained strong-motion records for forty-one actual buildings during five different earthquakes by using the normalized input output minimization (NIOM) method. This method can model wave propagation in multiple linear systems by considering the statistical correlation of the earthquake motions at different observation locations, and can reveal the arrival times of incident and reflected waves as well as their relative amplitudes. From these values, the fundamental period and the damping ratio of the building could be simply estimated. The estimated values were then compared with the values for the analytical building models, the values estimated in the previous studies for the actual buildings, and the building code formula.

Keywords: strong motion records; buildings; wave propagation; fundamental period; damping

1. Introduction

Records of building motion are a valuable source of experimental data containing all the uncertainties inherent in the behavior of buildings during earthquakes. However, the effects of ground motion on buildings cannot be directly seen from the records because they are much more complex than those during oscillator experiments (Ohba 1981). Therefore, after getting the records, they should be thoroughly analyzed.

Analyzing the behavior of a structure during an earthquake involves two problems: vibration and wave propagation, because the vibration of a structure results from seismic wave propagation in it. However, the most frequently used and conventional methodologies for studying building response to earthquake motions are the system identification method and spectral ratio analysis, which are vibration approaches. Vibration methods are well known and have been developed mainly for structural engineering purposes. In contrast, wave propagation approaches have mainly been used to investigate ground motions during earthquakes, and researchers have used several methods (such as impulse response and correlation functions) to simplify and clarify the wave propagation in soil layers and to determine soil properties.

This paper introduces an application of wave propagation modeling to the strong motion records for buildings. One of the wave propagation modeling methods is the normalized input output minimization (NIOM) method (Kawakami and Haddadi 1998, Haddadi and Kawakami 1998), and we use it in our study. The NIOM method models wave propagation in multiple linear systems by considering the statistical correlation of the earthquake motions at different observation locations.

First, the computed response time histories of the analytical building models are analyzed with the NIOM method in order to check the applicability of the method to building records. Next, actual acceleration records recorded in forty-one buildings during several recent earthquakes are analyzed and compared with the results for the analytical building models. Obtained wave arrival times and wave amplitude ratios are simply related to vibration properties like the fundamental period and damping ratio of each building. Finally, conclusions are drawn by comparing the NIOM results for the actual and analytical buildings with those of previous investigations.

2. Data

2.1 Computed Response of Assumed Analytical Building

The earthquake responses of six analytical buildings with 2, 5, 10, 20, 30 and 40 stories were computed. The fundamental periods of these buildings are assumed to be 0.5, 0.8, 1.6, 3.0, 4.0 and 5.0 s, respectively, based on previous research on the fundamental period of steel moment-resisting frame buildings. The buildings used in this paper are the same as in Chopra (1995), and all the stories of these buildings have equal masses (45.3 t) and heights (4 m). Figure 1(a) shows a 10-story building and its properties. The story stiffnesses for the other buildings are given in Fig. 1(b).

*Contact Author: Hideji Kawakami, Geosphere Research Institute of Saitama University, 255 Shimo-ohkubo, Sakura-ku, Saitama-shi, 338-8570 Japan
Tel: +81-48-858-3543 Fax: +81-48-858-3543
e-mail: kaw@kiban.civil.saitama-u.ac.jp
(Received November 8, 2003 ; accepted April 6, 2004)

The acceleration time history recorded in the basement of 3710 Wilshire Boulevard during the San Fernando earthquake of February 9, 1971 (National Geophysical Data Center 1996) was used as a motion at the ground surface (Fig. 2(a)). The responses of the assumed buildings were computed by modal analysis, in which a Rayleigh damping ratio of 5% was assumed in the first two modes (Chopra 1995). The ground motion and the computed response acceleration time histories at the fifth floor and roof are shown in Fig. 2(a). In order to check the applicability of the wave propagation modeling method to buildings, the computed responses were analyzed by the NIOM method.

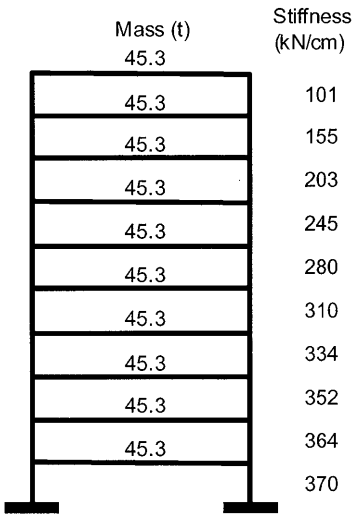

(a)

		20-story	30-story		40-story	
		20F-111	20F-333	30F-143	20F-447	40F-155
		19F-139	19F-348	29F-166	19F-457	39F-175
		18F-165	18F-362	28F-187	18F-466	38F-193
		17F-190	17F-375	27F-208	17F-474	37F-212
		16F-214	16F-387	26F-228	16F-482	36F-230
		15F-236	15F-399	25F-248	15F-490	35F-247
		14F-256	14F-410	24F-266	14F-497	34F-264
		13F-275	13F-420	23F-284	13F-503	33F-280
		12F-293	12F-429	22F-301	12F-509	32F-296
		11F-309	11F-437	21F-318	11F-514	31F-311
		10F-323	10F-445		10F-519	30F-326
		9F -337	9F -452		9F -524	29F-340
		8F -348	8F -458		8F -528	28F-354
	5-story	7F -359	7F -464		7F -531	27F-368
		6F -367	6F -468		6F -534	26F-381
	5F- 153	5F -375	5F -472		5F -537	25F-393
2-story	4F- 256	4F -380	4F -475		4F -539	24F-405
	3F- 334	3F -385	3F -478		3F -540	23F-416
2F- 224	2F- 386	2F -388	2F -479		2F -541	22F-427
1F- 336	1F- 412	1F -390	1F -480		1F -542	21F-438

(b)

Fig.1. (a) Configuration and Properties of Assumed 10-story Building and (b) Distribution of Story Stiffness in Assumed 2-, 5-, 20-, 30-, and 40-story Buildings (Chopra 1995)

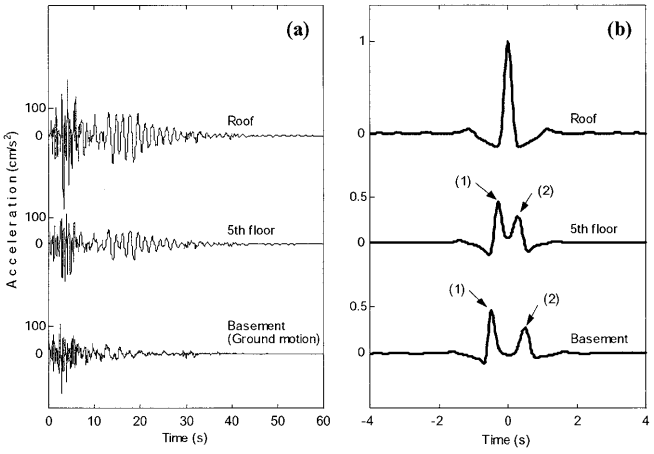

Fig.2. (a) Computed Response Acceleration of Assumed 10-story Building with Damping Ratio of 0.05 and (b) NIOM Method Analysis Result

2.2 Records for Actual Buildings

We analyzed strong-motion records of forty-one buildings: twenty-one buildings during the February 9, 1971 San Fernando earthquake, one building during the October 1, 1987 Whittier Narrow earthquake, four buildings during the October 19, 1989 Loma Prieta earthquake, thirteen buildings during the January 17, 1994 Northridge earthquake (all in California, USA), and two buildings during the January 17, 1995 Hyogo-ken Nanbu earthquake in Japan (National Geophysical Data Center 1996, CSMIP 1994, Architectural Institute of Japan 1996). However, due to the limited space, we have selected the four buildings shown in Table 1 to illustrate how the wave propagates in the building. Table 1 lists the building and earthquake names, epicentral distance, structural type, number of stories, and observed maximum accelerations at the basement and top floor of the four buildings.

Table 1. Building Specifications

No	Building	Earthquake & epicentral distance	Structural type and number of stories	Maximum recorded acceleration on the basement/ top floors	
				NS	UD
1	Transame-rica Bldg, San Francisco	Loma Prieta, 99 km	Steel frame, 60	0.11g/ 0.29g	0.05g/ 0.14g
2	20-story hotel, North Hollywood	Northridge, 21 km	Reinforced concrete frame, 20	0.3g/ 0.7g	--
3	1640 S. Marengo, Los Angeles	San Fernando, 41 km	Reinforced concrete, 7	0.12g/ 0.23g	0.08g/ 0.105g
4	8639 Lincoln Avenue, Los Angeles	San Fernando, 49 km	-- 11	0.03g/ 0.12g	0.04g/ 0.06g

3. Wave Propagation Modeling Method

The normalized input output minimization (NIOM) method used in this study can model wave propagation in multiple linear systems by considering the statistical correlation of earthquake motions at different observation locations. It can simplify the complex waveforms observed, extract several wave components such as incident and reflected waves, and give arrival times of incident and reflected waves as well as their relative amplitudes. Since the wave propagation velocity depends greatly on the characteristics of materials and structures through which the wave propagates, we have tried to apply such a method to building record analysis in addition to ground motion analysis. A brief review of the method is given below (Kawakami and Haddadi 1998, Haddadi and Kawakami 1998, Oyunchimeg and Kawakami 2003).

When a time-invariant linear system is subjected to earthquake motion, the input and outputs of the system in the frequency domain can be related by means of the transfer functions $H_l(\omega)$ (l=1,2,…,M). In the case of observed earthquake motions, the outputs at each frequency are given by

$$G_l(\omega_i)=H_l(\omega_i)F(\omega_i) \quad (l=1,2,\cdots,M) \tag{1}$$
$$(i=0,...,N-1 \text{ and } \omega_i=i\frac{2\pi}{N\Delta t})$$

where Δt = the sampling rate in the time domain; M = the number of output motions; N = the number of samples; and $F(\omega_i)$ and $G_l(\omega_i)$ = the Fourier transforms of the observed earthquake input and output motions, respectively.

It should be noted that input couldn't be separated from output in the analysis of a feedback system. In fact, all the observed motions can be considered as different outputs subjected to a common excitation. In this paper, the input motion means neither the incident-wave motion nor the excitation, but the motion observed at one arbitrary location (the building's roof in this paper).

Transfer functions depend only on the physical properties of the system. Therefore, the same transfer function as the one that defines the relationship between the observed input $F(\omega_i)$ and output $G_l(\omega_i)$ should satisfy the relationship between the simplified input model $X(\omega_i)$ and the simplified output model $Y_l(\omega_i)$.

$$Y_l(\omega_i)=H_l(\omega_i)X(\omega_i) \quad (l=1,2,\cdots,M) \tag{2}$$

The procedure leading to the simplified input and output models is shown schematically in Fig. 3. Here, the observed input $F(\omega_i)$ and output $G_l(\omega_i)$ are used to compute the transfer function $H_l(\omega_i)$. Minimizing the summation of the squared values of Fourier amplitude spectra of the input and outputs would result in the simplified input model, $X(\omega_i)$, and the simplified output models, $Y_l(\omega_i)$, (l=1,2,…,M). However, if there is not any constraint, the minimization procedure gives zero input and zero outputs at all times, and it does not give any useful result. Therefore, we assume that the amplitude of the input model at the building's roof at time $t=0$ is defined to be normalized to unity. The Lagrange multipliers method gives the following equation:

$$L=\sum_{i=0}^{N-1}\Bigg[\, c_0|X(\omega_i)|^2+k_0\omega_i^2|X(\omega_i)|^2 + \sum_{l=1}^{M}\left\{c_l|Y_l(\omega_i)|^2+k_l\omega_i^2|Y_l(\omega_i)|^2\right\}\Bigg] - \lambda\left\{\frac{1}{N\Delta t}\sum_{i=0}^{N-1}X(\omega_i)-1\right\} \tag{3}$$

where λ = Lagrange multiplier; c_0 to c_M = weighting constants of the squared Fourier amplitude spectra of the input and outputs; and k_0 to k_M = those of their time derivatives.

When the ratios of the two weighting constants (k and c) are chosen to be the same for the input and outputs ($k_0/c_0=k_1/c_1=\cdots=k_M/c_M$), the simplified input and output models are determined by the following equations.

$$X(\omega_i)=N\Delta t\frac{1}{\left\{1+\frac{k_0}{c_0}\omega_i^2\right\}\left(c_0+\sum_{m=1}^{M}c_m|H_m(\omega_i)|^2\right)}\Bigg/\sum_{n=0}^{N-1}\frac{1}{\left\{1+\frac{k_0}{c_0}\omega_n^2\right\}\left(c_0+\sum_{m=1}^{M}c_m|H_m(\omega_n)|^2\right)} \tag{4}$$

$$Y_l(\omega_i)=N\Delta t\frac{H_l(\omega_i)}{\left\{1+\frac{k_0}{c_0}\omega_i^2\right\}\left(c_0+\sum_{m=1}^{M}c_m|H_m(\omega_i)|^2\right)}\Bigg/\sum_{n=0}^{N-1}\frac{1}{\left\{1+\frac{k_0}{c_0}\omega_n^2\right\}\left(c_0+\sum_{m=1}^{M}c_m|H_m(\omega_n)|^2\right)} \tag{5}$$

The inverse Fourier transforms of Eqs. (4) and (5) give simplified input and output models in the time domain. This procedure is called the NIOM method.

Simplified models may not always represent what is happening physically in detail. However, because these models satisfy the statistical correlations between the observed motions, they help us to simplify and extract the physical properties of the system. The NIOM method offers the advantage of being able to investigate building responses using only observed earthquake motions without introducing any structural information like story stiffness or damping distributions. The capabilities and applicability of the method were presented previously by the developers (Kawakami and Haddadi 1998, Haddadi and Kawakami 1998).

$$\left.\begin{array}{l} f(t_i)\rightarrow F(\omega_i) \\ \text{Observation} \\ g_l(t_i)\rightarrow G_l(\omega_i) \end{array}\right\} \rightarrow \frac{G_l(\omega_i)}{F(\omega_i)} = H_l(\omega_i) \rightarrow \boxed{\text{NIOM}} \rightarrow \left\{\begin{array}{l} X(\omega_i)\rightarrow x(t_i) \\ \text{Simplified model} \\ Y_l(\omega_i)\rightarrow y_l(t_i) \end{array}\right.$$

Fig.3. Schematic Procedure of NIOM Method

4. Numerical Analysis

4.1 Analysis of Computed Response of Assumed Building

We applied the NIOM method to the computed response accelerations of a 10-story building, such as shown in Fig. 2(a), and obtained the simplified input and outputs as shown in Fig. 2(b). Here, the response acceleration at the roof was considered as the input, and the acceleration responses at the other nine floors were considered as outputs. Figure 2(b) shows analysis results when the sampling rate of the time series was 0.02 s and weighting constants were $k_0=0.01$, $c_0=1$ and $c_1=\ldots=c_9=1$. As shown in Fig. 2(b), the input was modeled such that its amplitude at time $t=0$ was unity and the amplitudes at the other times and output approached zero unless correlation existed between them. One may understand simply that the amplitude at the top story is assumed to be 1.0, and relative amplitude compared to the top story is obtained for the other stories.

One can see two clear peaks in the simplified output models corresponding to the incident and reflected waves, which are indicated by arrows (1) and (2) in the figure, respectively. The incident wave propagates from the basement to the roof, whereas the reflected wave propagates from the roof to the basement. Arrival times of the incident and reflected waves were the same: 0.28 s and 0.48 s at the fifth floor and basement, respectively. The waveforms of the simplified models changed as we changed the value of k_0, which determines the contribution of high or low frequencies (Haddadi and Kawakami 1998), but the obtained wave arrival times were similar. However, due to the limited space, only figures showing NIOM analysis results for $k_0=0.01$ are given in this paper.

Also, Fig. 2(b) shows that the reflected wave amplitude was smaller than the incident wave amplitude in the output models. The NIOM results for the assumed building were obtained by changing the damping ratio from 1% to 30%: cases of 1%, 5%, 10% and 20% damping are shown in Fig. 4. One can see that the difference between the incident and reflected wave amplitudes increased with increasing damping ratio, and that the arrival times were similar for different damping ratios.

4.2 Analysis of Actual Building Records

The analysis results obtained using horizontal components of the records in the selected buildings are shown in Fig. 5, when $k_0=0.01$, $c_0=1$, and $c_l=1$ (l=1, 2, ...). As seen from this figure, the simplified output models showed two peaks, the same as in the case of the analytical building in Figs. 2(b) and 4, and arrows (1) and (2) indicate incident and reflected waves, respectively. Arrival times of the incident and reflected waves for each floor are mostly the same. In Fig. 5, simplified output models for the actual building records show a smaller amplitude for the reflected wave than for the incident wave in all cases, the same as in the assumed building case in Fig. 4.

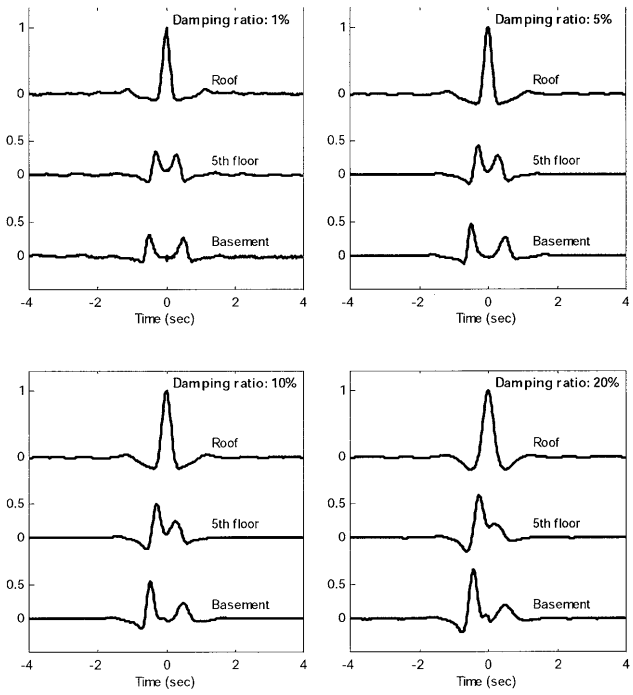

Fig.4. NIOM Analysis Results Using Computed Response of Assumed 10-story Building with Different Damping Ratios

5. Discussion of Analysis Results

Simplified models obtained from the NIOM method give the arrival time and relative amplitude of incident and reflected waves at each level. Some interpretation of these results is needed to obtain the dynamic characteristics of the structure, as discussed below.

5.1 Wave Arrival Time and Fundamental Period

Arrival times of incident and reflected waves at the basement/ground floor (which are equal to the wave travel times through the height of the building) are plotted in Fig. 6 for the analytical and actual buildings. One can see that these were very similar except for a few cases. This indicates the reliability of the NIOM method.

The question is what is the relationship between the

fundamental period and wave travel time through the building. As we know, the fundamental frequency of a uniform soil deposit is given by $\omega_0=\frac{\pi v_s}{2H}$, and the corresponding period is $T=\frac{2\pi}{\omega_0}=\frac{4H}{v_s}=4\tau$, where H= thickness of the soil deposit; v_s= shear wave velocity; and τ= wave travel time through the soil deposit. Corresponding to the non-uniform building model shown in Fig. 1(a) [case 1 in Fig. 7], we assumed a 10-story uniform building with the same stiffness of 230 kN/cm in all stories (case 2 in Fig. 7). This value of K=230 kN/cm was chosen by assuming a series spring system: $\sum_{i=1}^{10}\frac{1}{K_i}=\frac{10}{K}$, where K_i= stiffness of each story in case 1 (see Fig. 1(a)) and K= story stiffness (same in all stories) in case 2.

Figure 8 shows the NIOM analysis results for cases 1-3 in Fig. 7. As shown in case 2 in Figs. 7 and 8, the obtained value of $T=4\tau=4\times0.48=1.92$ s for this uniform building model deviates by about 3% from the fundamental period T=1.86 s calculated from the smallest eigenvalue in the modal analysis. However, in the case of the analytical building shown in Fig. 1(a), i.e., case 1 in Figs. 7 and 8, $T=4\tau=4\times0.48=1.92$ s, while the fundamental period obtained by modal analysis was 1.60 s. Case 3 of the story stiffness distribution, where the order of story stiffness is reversed from that in case 1, gave $T=4\tau=4\times0.48=1.92$ s, while the fundamental period obtained by modal analysis was T=2.11 s.

It is interesting that the wave travel times τ are equal to 0.48 s in all three cases, but the fundamental periods differ from case to case. This means that the arrival time obtained from the NIOM method is precisely the wave travel time from the basement to the roof. The wave travel time is used in the wave propagation problem, and it has a different meaning from the fundamental period, which is used in the vibration problem. We can say that four times the wave travel time τ, $T=4\tau$, gives a reliable value of the fundamental period for a fairly uniform or low-rise building. However, the value of $T=4\tau$ is overestimated (underestimated) compared with modal analysis when story stiffness is decreased (increased) from basement to roof.

Figure 9 shows relationships between building height and the value of $T=4\tau$ (fundamental period) for the assumed buildings in Fig. 1 and several actual buildings (NS components) in comparison with the empirical formula from the Uniform Building Code. The empirical

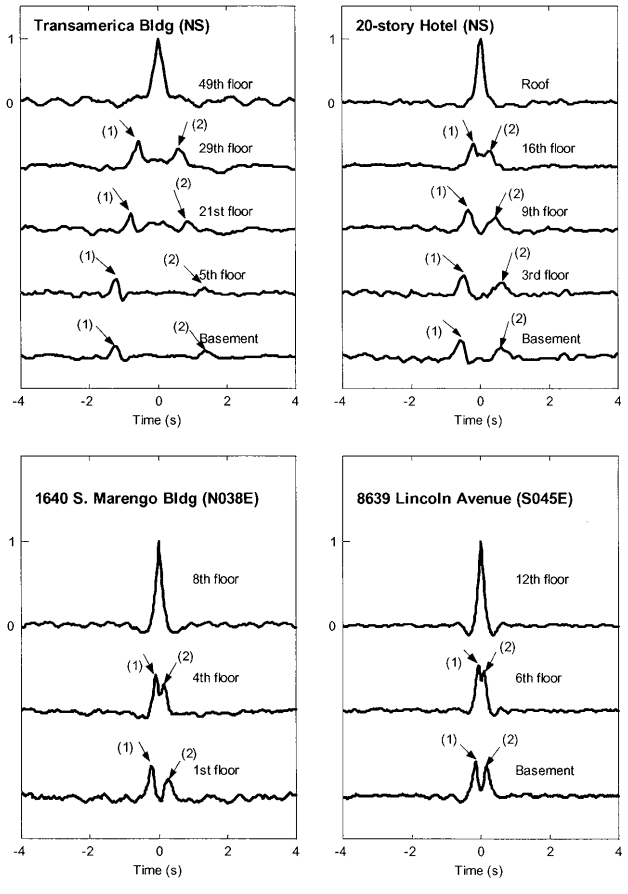

Fig.5. NIOM Results for Actual Building Records (Horizontal Component)

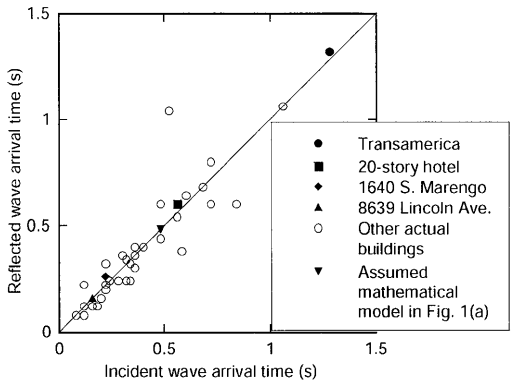

Fig.6. Relationships between Arrival Times of Incident and Reflected Waves (NS Component)

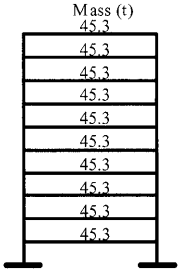

		Story stiffness (kN/cm)		
		Case 1	Case 2	Case 3
		101	230	370
		155	230	364
		203	230	352
		245	230	334
		280	230	310
		310	230	280
		334	230	245
		352	230	203
		364	230	155
		370	230	101
Fundamental period (s)	NIOM method $T=4\tau$	1.92	1.92	1.92
	Modal analysis	1.60	1.86	2.11

Fig.7. Fundamental Periods Obtained by Two Methods for Assumed 10-story Buildings

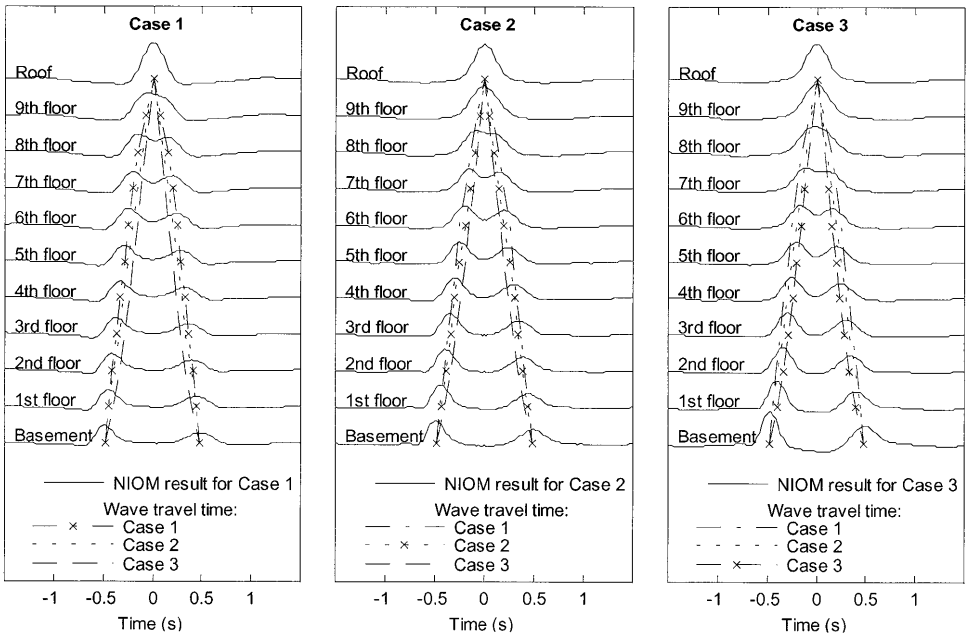

Fig.8. NIOM Analysis Results for Cases 1-3 of 10-story Building in Fig. 7

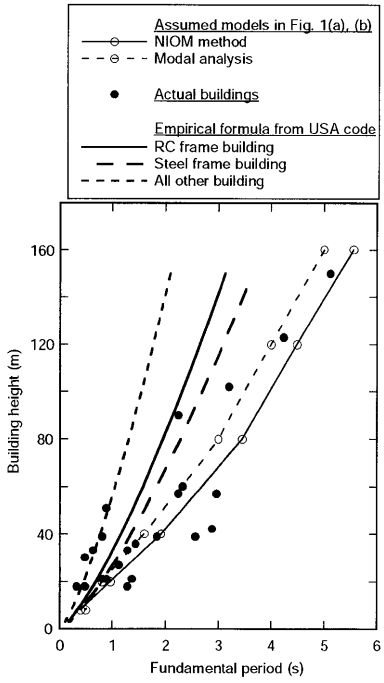

Fig.9. Relationships between Building Height and Fundamental Period ($T=4t$) (NS Component)

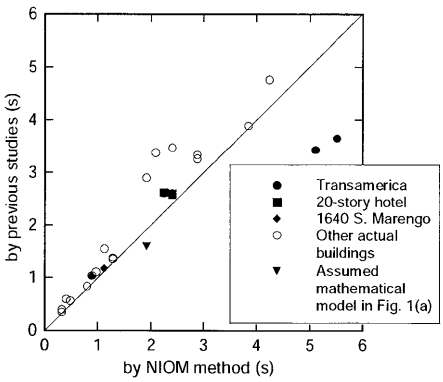

Fig.10. Comparisons of Fundamental Periods of Buildings Obtained by NIOM Method and Previous Studies

formula for estimating the fundamental period of different types of buildings is $T=ah^{3/4}$, where $a=0.0731$, 0.0853, and 0.0488 for reinforced concrete moment-resisting frames and eccentrically braced frames, steel moment-resisting frames, and all other buildings, respectively; and $h=$ building height in meters (ICBO 1997).

Fundamental periods ($T=4\tau$) obtained from incident wave arrival times in Fig. 5 were 5.12 (5.28) s for the Transamerica building (NS component), 2.24 (2.4) s for the 20-story hotel (NS component), 0.88 (0.88) s for 1640 S. Marengo (N038E component), and 0.64 (0.64) s for 8639 Lincoln avenue (S045E component) [values in parentheses indicate the periods obtained from reflected wave arrival times]. The differences between periods obtained from incident and reflected waves are less than 10%, and they may be because of the wide peaks in Fig. 5. Meanwhile, the fundamental periods determined by previous investigations were 3.4 s for the Transamerica building (Safak and Celebi 1991), 2.62 s for the 20-story hotel (Goel and Chopra 1997), and 1.03 s for 1640 S. Marengo (Hart and Vasudevan 1975).

Figure 10 compares the fundamental periods obtained by the NIOM method with those obtained by previous researchers for both the NS and EW components. Other actual buildings marked (open circle plots) include two buildings studied by Celebi (1992), five buildings by

Goel and Chopra (1997), and three buildings by Hart and Vasudevan (1975); our results show relatively good agreement with those of the previous studies.

One may think that errors in estimating fundamental periods in Fig. 7 are sizable and that the story stiffness distribution can be used to modify the estimated values ($T=4\tau$). One may also think that from the differences in the fundamental period shown in Fig. 7, the differences between the NIOM and the previous studies should be larger than those obtained in Fig. 10. This discrepancy may be explained by taking the soil-structure interaction into consideration.

5.2 Wave Amplitude and Damping Ratio

Figure 11 shows the relationships between incident and reflected wave amplitudes at the basement in the analytical and actual buildings (see Figs. 2(b) and 5). The amplitude of the reflected wave is clearly smaller than that of the incident wave, and this result can be explained by the damping of the structure.

In order to clarify the effect of damping ratio on the wave amplitude, we analyzed the analytical buildings for various damping ratios. The difference between incident and reflected wave amplitudes increased with increasing damping ratio, as shown in Fig. 4, which shows the case of the 10-story building. Figure 12 shows the relationship between damping ratio and wave amplitude ratio (reflected to incident) at the basement for the 2-, 5-, 10-, 20-, 30-, and 40-story analytical buildings, which reveals a clear relationship between the two ratios. Therefore, the wave amplitude ratio obtained by the NIOM method can be used to estimate the damping ratio of the building.

Figure 13 shows the wave amplitude ratio versus building height for analytical buildings with damping ratios of 1, 2, 3, 4, 5, 10, 20 and 30%. The values for several actual buildings are also plotted. The damping ratio for each actual building can be estimated by comparing the plot with the curves for different damping ratios. One can see that most of the actual buildings fall between curves corresponding to 1% and 10% damping, which is consistent with the recommended values of damping ratio for various types of buildings. The figure also has plots for buildings with damping ratios from 0% to 5% used in previous studies (Safak and Celebi 1991, Goel and Chopra 1997, Hart and Vasudevan 1975, Celebi 1992) indicated by open circles, 5% to 10% indicated by open squares, 10% to 15% indicated by open rhombuses, and more than 15% indicated by open triangles. Crosses in this figure correspond to buildings whose damping ratios were not available from the previous studies.

One might think that the damping ratio of 10 % or higher appears to be too large for ordinary buildings if the soil-structure interaction is not considered. One may also think that Fig. 13 shows that the damping ratios obtained by the NIOM method do not agree well with those obtained by the previous methods and that the damping ratio estimation may be improved by considering the ratio of wave amplitude decay to the wave propagation distance. Further study on this issue should be conducted in the future. However, we should notice that the damping ratio has been difficult to estimate accurately and that the estimated value depended greatly on the method used.

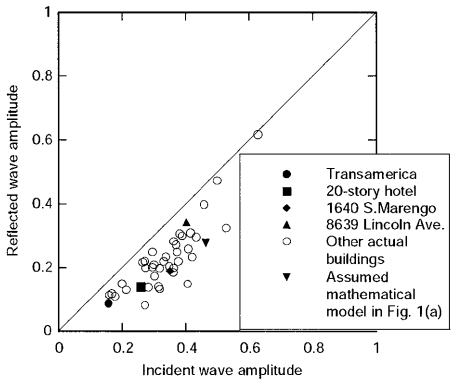

Fig.11. Relationships between Incident and Reflected Wave Amplitudes (NS Component)

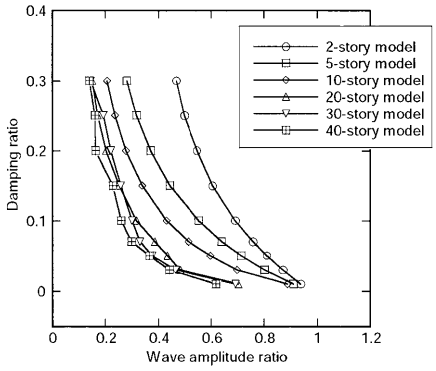

Fig.12. Relationships between Wave Amplitude Ratio and Damping Ratio for Assumed Multistory Buildings

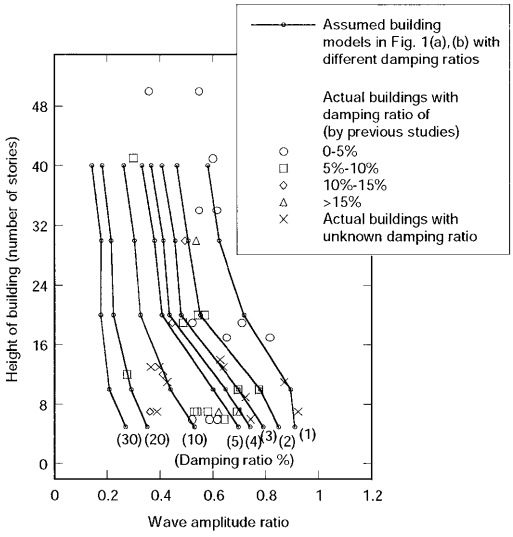

Fig.13. Relationships between Building Height, Wave Amplitude Ratio, and Damping Ratio

6. Conclusions

This paper introduced an application of the wave propagation modeling method, i.e., the NIOM method, to clarify how seismic waves propagate through a building during an earthquake and to relate the obtained results to the dynamic properties of the building. Our main conclusions are as follows.

1) The NIOM method gave results with two clear peaks in the outputs, corresponding to incident and reflected waves propagating vertically in the building. Such results were similar for all the analyzed actual buildings, which were of various structural types and materials.
2) The arrival time τ at the basement was precisely the wave travel time from the basement to the roof. Arrival times of the incident and reflected waves were mostly the same.
3) The wave travel time as calculated by the NIOM method has a different meaning from the fundamental period, which is used in the vibration problem. The value 4τ gives an approximate value of the fundamental period for a uniform or low-rise building. However, it overestimates (underestimates) the fundamental period when story stiffness is decreased (increased) from basement to roof.
4) Reflected wave amplitude was always smaller than incident wave amplitude, and the ratio of the amplitudes can be used to estimate the damping ratio.

Acknowledgements

We are grateful to the National Geophysical Data Center, Colorado; California Strong Motion Instrumentation Program, California Department of Conservation, Division of Mines and Geology of the USA; and Architectural Institute of Japan for providing the earthquake strong-motion records used in our study.

References

1) Architectural Institute of Japan (1996) Collected strong motion records from 1995 Hyogo-ken Nanbu earthquake. Tokyo, Japan.
2) California Strong Motion Instrumentation Program (CSMIP) (1994) Processed data from the Northridge Earthquake of 17 January 1994. Report OSMS 94-11, California.
3) Celebi, M. (1992) Highlights of Loma Prieta responses of four tall buildings. Proceedings of Earthquake Engineering, Tenth World Conference, Balkema, Rotterdam.
4) Chopra, A. K. (1995) Dynamics of structures: Theory and applications to earthquake engineering. Prentice Hall, Inc., NJ.
5) Goel, R. K. and Chopra, A. K. (1997) Vibration properties of buildings determined from recorded earthquake motions. Rep. No. UCB/EERC-97/14, Earthquake Engineering Research Center, University of California at Berkeley.
6) Haddadi, H. R. and Kawakami, H. (1998) Modeling wave propagation by using normalized input-output minimization (NIOM) method for multiple linear systems. *Journal of Structural Mechanics and Earthquake Engineering*, JSCE 584/I-42, 29-39.
7) Hart, G. C. and Vasudevan, R. (1975) Earthquake design of buildings: Damping. *Journal of the Structural Division*, ASCE, 11-30.
8) International Conference of Building Officials (ICBO). 1997. Uniform building code. Whittier, California.
9) Kawakami, H. and Haddadi, H.R. (1998) Modeling wave propagation by using normalized input output minimization (NIOM). *Soil Dyn. and Earthquake Engrg.*, 17, 117-126.
10) Kramer, S.L. (1996) Geotechnical earthquake engineering. Prentice Hall, Inc., NJ.
11) National Geophysical Data Center (1996) Earthquake strong motion 3-volume CD-ROM collection. Boulder, Colorado.
12) Newmark, N.M. and Hall, W.J. (1982) Earthquake spectra and design. Earthquake Engineering Research Institute, Berkeley, California.
13) Ohba, S. (1981) Wave propagation in buildings during oscillator experiment, AIJ Annual Meeting, 849-850 (in Japanese).
14) Osaki, M. (1990) Vibration theory of buildings. Syokoku-sha, Tokyo (in Japanese).
15) Oyunchimeg, M. and Kawakami, H. (2003) A new method for propagation analysis of earthquake waves in damaged buildings: evolutionary normalized input-output minimization (NIOM). *Journal of Asian Architecture and Building Engineering*, 2(1), 9-16.
16) Safak, E. and Celebi, M. (1991) Seismic response of Transamerica building. II: System Identification. *Journal of Structural Engineering*, ASCE, 117(8), 2405-2425.